2005 American Control Conference
June 8-10, 2005. Portland, OR, USA

Robust Control of a Morphing Airfoil Structure

Christopher E. Whitmer
Corresponding author, Graduate student
Mechanical Engineering
Iowa State University
Ames, Iowa 50011
Email: whitmer@iastate.edu

Atul G. Kelkar
Associate Professor
Mechanical Engineering
Iowa State University
Ames, Iowa 50011
Email: kelkar@iastate.edu

***Abstract*— This paper presents several robust control designs for a MIMO morphing airfoil concept. A linear aeroelastic model of the morphing wing is utilized to design an H_∞ controller and a two degree of freedom H_∞ loop shaping controller that track commanded lift and roll moments. These methodologies are developed, along with the robustness conditions for input multiplicative, and real parametric uncertainty in ω_n and ζ_n. The robustness of each of these controllers is then evaluated using these conditions and the structured singular value (SSV). Comments and discussion on these control methodologies are then drawn presented.**

I. INTRODUCTION

In recent years, considerable research effort and resources have been invested to assess the viability and/or realizability of biologically inspired flight systems. The goal of most of these research efforts has been to model, control, and develop "morphing" aerodynamic structures composed of large numbers of sensors and actuators. Such morphing wing designs could be utilized to achieve many performance objectives from flutter suppression to flight control. Several approaches to this problem including but not limited to [3], [2], [5] and [1] have utilized aeroelastic deformations used to control aerodynamic quantities. The efforts of this project build apon these strategies. The stability and performance of this airfoil are highly dependant on shape. Consequently if there are uncertainties in the model (which is significantly more complicated than a traditional airfoil) the stability and performance of the airfoil control mechanism is less robust than traditional airfoils. A finite dimensional linear aeroelastic model of a scale morphing wing was previously obtained in [1]. Under the right conditions this design model is an accurate representation of an aeroelastic morphing wing. However, even with accurate system ID information a number of uncertainties will creep into the closed loop system. For example, uncertainties in the input control signal to the plant, uncertainties in the identified modal parameters of the aeroelastic system, and uncertainties due to plant dynamics neglected for the controller design could all destabilize a nominally stable closed loop or adversely affect the performance of the closed loop system. The goal of this paper is to investigate potential robust control strategies for this control design model and evaluate them based on robustness, performance, and ease of application to this type of system.

II. MODEL

The wing geometry used is the NACA series 2415 airfoil. The finite element structural model was created in FEMLAB, a Matlab toolbox, and a static aerodynamic model using vortex lattice method was developed. The aerodynamic and structural models were then combined and a finite dimensional linearized model of the wing structure was constructed. The details of this procedure may be found in [1]. In condensed notation, the aeroelastic equation becomes:

$$\ddot{q}(t) + \left(\tilde{\mathcal{C}} + \mathcal{F}\right)\dot{q}(t) + (\Omega + \mathcal{K})\,q(t) = \mathcal{B}_z\vec{F_c} + \mathcal{B}_\alpha\alpha \quad (1)$$

Where $q(t)$ is the generalized modal coordinate, Ω is the diagonal matrix of structural natural frequencies, $\tilde{\mathcal{C}}$ is the structural damping, $\mathcal{F}$ is the aeroelastic damping, $\mathcal{K}$ is the aeroelastic stiffness, and the terms $\vec{F_c}$ and α are actuator and angle of attack inputs. In a $2*n$ dimensional state space representation (with n equal to the desired number of modes in the model). This has the form shown in equation (2).

$$\begin{gathered}\dot{x}(t) = Ax(t) + B_u u(t) + B_w w(t) \quad y(t) = Cx(t) \\ y_{prf}(t) = C_{prf}x(t) + D_u u(t) + D_w w(t)\end{gathered} \quad (2)$$

In this expression, the matrix A is composed of both a second order diagonal form from the structural equations and the aeroelastic interaction terms $\mathcal{K}$ and $\mathcal{F}$ from the aerodynamic model. Matrices B_u, B_w, and C have the form:

$$B_u = \begin{bmatrix} 0 \\ \mathcal{B}_{z(1,1:p)} \\ \vdots \\ 0 \\ \mathcal{B}_{z(n,1:p)} \end{bmatrix}; \quad B_w = \begin{bmatrix} 0 \\ \mathcal{B}_{\alpha(1,1:p)} \\ \vdots \\ 0 \\ \mathcal{B}_{\alpha(n,1:p)} \end{bmatrix}$$

$$C = \begin{bmatrix} \Phi_{ui} & 0 & \ldots & \Phi_{un} & 0 \end{bmatrix}$$

In this case, C corresponds to the z-displacement as output and Φnn are portions of the mode shape matrix.

Aerodynamic relationships for the performance outputs (lift and roll moment) were represented in terms of modal coordinates and C_{prf}, D_u, and D_w were constructed refer to [1] for details.

$$y_{prf}(t) = \begin{bmatrix} L_a(t) \\ M_R(t) \end{bmatrix} = \begin{bmatrix} \mathcal{G}_L\vec{q} + \mathcal{E}_L\vec{q} \\ \mathcal{G}_{M_R}\vec{q} + \mathcal{E}_{M_R}\vec{q} \end{bmatrix} + \begin{bmatrix} \mathcal{D}_{z_L}\vec{F_c} \\ \mathcal{D}_{z_M}\vec{F_c} \end{bmatrix} + \begin{bmatrix} \mathcal{D}_{\alpha_L}\alpha \\ \mathcal{D}_{\alpha_M}\alpha \end{bmatrix} \quad (3)$$

$$C_{prf} = \begin{bmatrix} \mathcal{E}_{L1} & \mathcal{G}_{L1} & .. & \mathcal{E}_{Ln} & \mathcal{G}_{Ln} \\ \mathcal{E}_{M_R1} & \mathcal{G}_{M_R1} & .. & \mathcal{E}_{M_Rn} & \mathcal{G}_{M_Rn} \end{bmatrix}$$
$$D_u = \begin{bmatrix} \mathcal{D}_{z_L} \\ \mathcal{D}_{z_M} \end{bmatrix} \quad D_u = \begin{bmatrix} \mathcal{D}_{\alpha_L} \\ \mathcal{D}_{\alpha_M} \end{bmatrix} \tag{4}$$

In addition to the aeroelastic model first order actuator dynamics were also added to the system. The state space representation of the combined system (neglecting disturbance input) is given in equation (6).

$$\begin{aligned} \dot{x_a}(t) &= A_a x_a(t) + B_v v(t) \\ u(t) &= C_a x_a(t) + D_v v(t) \end{aligned} \tag{5}$$

$$\begin{aligned} \begin{matrix} \dot{\vec{x}}(t) \\ \dot{\vec{x}}_a(t) \end{matrix} &= \begin{bmatrix} A & B_u C_a \\ 0 & A_a \end{bmatrix} \begin{matrix} \vec{x}(t) \\ \vec{x}_a(t) \end{matrix} + \begin{bmatrix} 0 \\ B_v \end{bmatrix} v(t) \\ y_{prf}(t) &= \begin{bmatrix} C_{prf} & D_u C_a \end{bmatrix} \begin{matrix} \vec{x}(t) \\ \vec{x}_a(t) \end{matrix} \end{aligned} \tag{6}$$

The actuator representations used were first order transfer functions with a bandwidth of 170Hz and a $0dB$ DC gain.

III. CONTROL DESIGN METHODOLOGIES

This section presents development and designs of several different types of robust controllers. Two different controller types considered included H_∞, and two degree of freedom McFarlane- Glover H_∞ loop shaping controllers. The development of the robust stability and performance conditions to additive, input multiplicative, and real parametric uncertainties are also included.

A. H_∞ Synthesis Formulation

H_∞ design provides a systematic approach to design for uncertainties in the model as well as the ability to include performance objectives in the design (for example tracking and control energy). The control law is obtained as a solution to an optimization problem which incorporates objectives like bandwidth, roll-off, and resolution into its cost function. The robust stability of H_∞ controllers to uncertainty arises from the small gain theorem. In the following paragraphs the H_∞ method will be developed in greater detail.

If it is desired to minimize the disturbance input $d(t)$ the sensitivity function S should be made much less than one. Likewise, if it is desired to have good tracking the complementary sensitivity T should be I at all frequencies and if it is desired that we minimize the noise we should make T small at all frequencies. Since $S + T = I$ it is not possible to satisfy all these requirements in all frequency ranges. However, in most systems (including this one) it is only necessary to lessen low frequency disturbances, track in low frequencies, and reject noise in high frequencies. This allows T to be nearly identity (and S to be nearly zero) in the low frequencies and T to be nearly zero (and S to be nearly one). By selecting appropriate weights on S and T these constraints, as well as constraints imposed by robust stability (section III-C) may be accommodated. These same concepts are applicable in H_∞. The first step towards H_∞ synthesis is to formulate the generalized plant for the feedback system by identifying the exogenous inputs, the control inputs, the error signals, and the exogenous outputs that are indicators of the desired performance constraints. The standard H_∞ representation weights the error signal ($Z_1(s) = W_P E(s)$), the control signal ($Z_3(s) = W_U U(s)$), and the measured output signal ($Z_2(s) = W_T Y(s)$). The map from $R(s)$ to $Z_1(s)$ is the weighted sensitivity function, $W_P S$. This transfer function can be thought to characterize the performance objective of good tracking. Similarly, the transfer function from $R(s)$ to $Z_2(s)$ is the weighted complementary sensitivity function, and characterizes measurement noise rejection. Lastly from $R(s)$ to $Z_3(s)$ is KS, which weights the control effort. The greatest effort of an H_∞ design is to select weight functions W_P, W_U, and W_T that impart frequency-dependent weights on the respective transfer functions to achieve the performance and robustness objectives. The transfer function, W_P, is chosen such that it has high gains at low frequencies and low gains at high frequencies. This weighting influences the optimal feedback law in such a way that the sensitivity function is small in the low frequency range. This ensures good tracking over the desired bandwidth. The weighting function W_T is a form which has low gains at low frequencies and higher gains at high frequencies because noise is generally a high frequency phenomenon. The transfer function KS is weighted by W_U, to restrict the magnitude of the control input signals such that they are representative of real actuators and saturation limits. In general this weight is a constant so as to keep the overall order of the controller as low as possible. With the generalized plant P as described by equation (7) and the stated H_∞ constraints it is possible to formulate an H_∞ problem. This problem is to design the otpimal controller K, such that the above listed constraints are satisfied.

$$\begin{bmatrix} z \\ v \end{bmatrix} = \underbrace{\begin{bmatrix} \begin{bmatrix} W_P & -W_P G_u \\ 0 & W_T G_u \\ 0 & W_U \end{bmatrix} \\ \begin{bmatrix} I - G_u \end{bmatrix} \end{bmatrix}}_{=P} \begin{bmatrix} r \\ u \end{bmatrix}$$

However, this particular problem is a difficult one to solve. It is computationally simpler to design a suboptimal controller (i.e. one that is close to but not the same as the optimal controller with respect to the H_∞ norm). Additionally, it is only possible to solve this problem with the standard H_∞ algorithm when formulated as the stacked problem in equation (7).

$$\left\| \begin{matrix} W_P S \\ W_T T \\ W_U K S \end{matrix} \right\|_\infty \leq 1 \tag{7}$$

B. Two DOF Formulation

With two degree of freedom control problems such as this one simply leaving one degree of freedom out of the design, as in the previous section, may be insufficient. In this case a two degree of freedom (DOF) McFarlane-Glover approach is desirable. This approach improves the model matching abilities of the closed loop. In [7] this approach illustrated in figure (1), is presented in greater detail. The control design

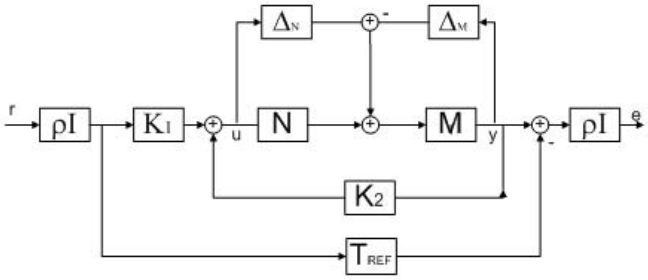

Fig. 1. Block diagram for 2 DOF McFarlane-Glover Design

problem is then to find a controller $K = [K_1 \quad K_2]$ that minimizes the H_∞ norm of the transfer matrix depicted in equation (8).

$$\begin{bmatrix} \rho(I - K_2G)^{-1}K_1 & K_2\chi M^{-1} \\ \rho\chi G K_1 & \chi M^{-1} \\ \rho^2[\chi G K_1 - T_{ref}] & \rho\chi M^{-1} \end{bmatrix}$$
$$\chi = (I - GK_2)^{-1} \tag{8}$$

This prefilter ensures that

$$\|(I - GK_2)^{-1}GK_1 - T_{ref}\|_\infty \leq \gamma\rho^{-2} \tag{9}$$

Where T_{ref} is the desired closed loop transfer function for model matching, and ρ is a parameter that reflects the relative importance of model matching and robust stabilization. A key difference between the one degree of freedom situation and the two degree of freedom situation is that gamma iterations are required to solve this problem. In fact the solution of this problem involves the use of a standard H_∞ algorithm. All that is required is to formulate the generalized plant and follow a traditional H_∞ procedure. If G and T_{ref} have state space representations $G(A_g, B_g, C_g, D_g)$ and $T_{ref}(A_t, B_t, C_t, D_t)$ then the generalized plant P has a state space representation given by equation (10).

$$\left[\begin{array}{ccc|cc} A_g & 0 & 0 & (B_gD_g^T + ZC_g^T)R^{\frac{-1}{2}} & B_g \\ 0 & A_t & B_t & 0 & 0 \\ \hline 0 & 0 & 0 & 0 & I \\ C_g & 0 & 0 & R^{\frac{1}{2}} & D_g \\ \rho C_g & -\rho^2 C_t & -\rho^2 D_t & \rho R^{\frac{1}{2}} & \rho D_g \\ 0 & 0 & \rho I & 0 & 0 \\ C_g & 0 & 0 & R^{\frac{1}{2}} & D_g \end{array}\right] \tag{10}$$

where $R = (I + D_gD_g^T)$ and Z is the solution of an Ricotti Equation [7].

C. Robust Stability Analysis

Robust analysis techniques were used to analyze the wing system. Input multiplicative uncertainty and real parametric uncertainty in natural frequencies and damping were investigated. To develop input multiplicative uncertainty, begin with the standard P-K-Δ description and use a lower linear fractional transformation P (plant) and K (controller) to yield N_{ydwd}. Then, the infinity norm of N_{ydwd} is bounded by one. The advantage of this $PK\Delta$ framework is that many types of uncertainties can be analyzed in the same way. The only difference between the additive and the input multiplicative characterizations lie in the exact form of N_{ydwd}. The form resulting in the input multiplicative

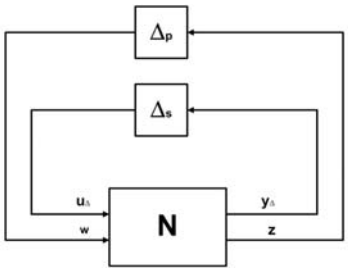

Fig. 2. Block diagram of the robust performance problem

expression of uncertainty yields the following sufficient condition.

$$\| W_iC(I + G_oC)^{-1}G_o \|_\infty \leq 1 \tag{11}$$

W_i is a diagonal constant weighting matrix where the constant is a percentage expression of the input signal (i.e. 0.25 for 25% uncertainty). This condition is then used to analyze the robustness of the system.

D. μ-analysis of Robust Stability and Performance

MIMO robust performance analysis makes use of the structured singular value (SSV). The robust stability problem and the robust performance problem are similar and the robust performance problem may be represented as a robust stability problem by using a Δ block of the form in figure(2). Let a nominal system M and perturbations Δ be stable. Then, the M-Δ system is stable for all allowed perturbations with $\bar{\sigma}(\Delta) \leq 1, \quad \forall\omega$ if and only if

$$\mu(M(j\omega)) < 1, \quad \forall\omega \tag{12}$$

Because robust stability and robust performance are similar the μ-analysis for robust performance is nearly the same as for robust stability. For the system in figure (2) if N is internally stable then

$$RP \Leftrightarrow \|\mathcal{F}_u(N, \Delta_s)\|_\infty < 1 \quad \leq 1 \Leftrightarrow \mu_{\hat{\Delta}}(N(j\omega)) < 1 \quad \forall\|\Delta_s\|_\infty\forall\omega \tag{13}$$

Where the structured singular value μ is computed with respect to the following Δ-block, with Δ_p a full complex perturbation matrix.

$$\hat{\Delta} = \begin{bmatrix} \Delta_s & 0 \\ 0 & \Delta_p \end{bmatrix} \tag{14}$$

Analysis with the properly structured Δ using equation (13) can provide a tighter bound than would be possible using an H_∞ bound. Additionally using the N-Δ form of figure (2), robust stability, and nominal performance may be restated. Robust stability is ensured when $\mu(N_{11}(j\omega)) < 1, \quad \forall\omega$. Lastly, nominal performance is ensured when N is nominally stable and $\bar{\sigma}(N_{22}(j\omega) < 1, \quad \forall\omega$.

Real paramentric uncertainty in this paper represents a real uncertainty in the frequency and damping of each of the aeroelastic modes. Under a transformation to companion form, these individual uncertainties ($\omega_{\delta i}$ and $\zeta_{\delta i}$) are present

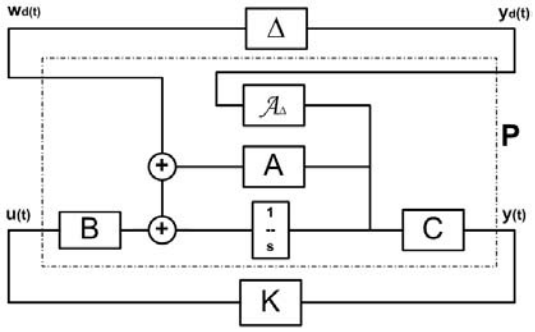

Fig. 3. PKΔ form for parametric uncertainty in the plant

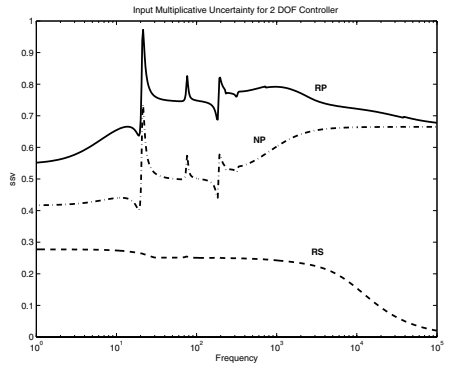

Fig. 4. SSV plots (H_∞ 2DOF design for Multiplicative Uncertainty)

only in elements a_{21} and a_{22} of each decoupled modal block. Consider the following example:

$$A_n = \begin{bmatrix} 0 & 1 \\ -(\omega_n + \omega_{\delta n})^2 & -2(\omega_n + \omega_{\delta n})(\zeta_n + \zeta_{\delta n}) \end{bmatrix} \quad (15)$$

Next, expand this expression and define the A matrix uncertainties a_{21} and a_{22}. Then, express these uncertainties as a weighing matrix multiplied into a diagonal real Δ block who's infinty norm is less than 1, all of which is in parallel to the nominal A matrix.

$$A = \begin{bmatrix} 0 & 1 \\ -\omega_n^2 & -2\omega_n\zeta_n \end{bmatrix} + \begin{bmatrix} 0 & 0 \\ \tilde{a}_{21} & \tilde{a}_{22} \end{bmatrix} \begin{bmatrix} \delta_1 & 0 \\ 0 & \delta_2 \end{bmatrix} \quad (16)$$

In this paper however only a set percentage uncertainty in all ω_n or all ζ_n parameters will be considered. A block diagram describing this interconnection and displaying the $P_o - K - \Delta$ configuration is shown in figure 3. The $\mathcal{A}_\Delta$ matrix is an n-mode weighting matrix.

E. H_∞ Design for Robust Stability

When considering the input multiplicative uncertainty case, the expression for N_{ydwd} is given in equation(11). This condition is the same as $W_i T_I$. However in the stacked H_∞ problem presented earlier there are no maps from any input to any output that equal T_I. Note that in SISO this is not a problem since $T = T_I$. A method that can allow design for robust stability to multiplicative uncertainty is to use a higher order weight on KS. This can work in some cases due to the fact that $T_I = KSG$. In this particular case using a constant W_u always yields an N_{ydwd} that has a spike that is larger than one. This clearly means that the system will not be robustly stable, however it also provides insight as to how to design a higher order weight on KS that drastically reduces N_{ydwd} at a particular frequency.

IV. SIMULATIONS

Several controllers were designed to control the morphing of the MIMO wing to achieve desirable aerodynamic performance. First order actuators were chosen to keep the overall size of the control design model small. The sensors are assumed to be accelerometers whose signals are integrated twice to yield displacements. The actuators and sensors are assumed to be in a nearly collocated configuration. The commanded references for tracking are lift and roll moment, and a prefilter was utilized to achieve a desired tracking performance for the single degree of freedom designs. All controllers presented were either designed, or tuned using robustness analysis to achieve good robustness.

A. Two DOF McFarlane-Glover Design

Coprime uncertainty has been shown in [4] to relate well to real paramentric variations in ω_n and ζ_n. A two DOF McFarlane-Glove Design, which was developed in section (III-B), should be able to yield good results. Pre and post compensators W_1 and W_2 were applied to shape the plant before the robustifying controller was designed. The resulting controllers should exhibit desired tracking responses, and have excellant robustness properties.

In the design for robustness to input multiplicative uncertainty W_2 was again chosen to be identity. W_1 was designed such that G_s would have an high gain at low frequency, S would have a desired bandwidth (greater than 150 Hz), and such that the singular values of S were small at low frequency. The diagonal first order transfer matrix that accomplishes this is:

$$W_1 = diag(\frac{0.1433s + 182.4}{s + 8.482})_{15\times 15} \quad (17)$$

The specified model matching parameter was $\rho = 3.6$ and the final $\gamma = 3.97$. The resulting controller has 44 states so controller reduction is preformed by a balanced residualization to leave 29 states. The singular value plots of S and T did satisfy the imposed constraints but plots have been omitted to conserve space. The reference step response, z displacement, and control signal verses time are given in the following figures. The tracking, z-displacement, and control signal responses are excellent and have been omitted for conciseness. The percentage uncertainty considered was 25% and this condition on $N_{ydwd} \ll 1$ was satisfied. The structured singular value plots in figure (4) are all below 1 indicating that the system has both robust performance and robust stability under this uncertainty description.

In the design for parametric Uncertainty the post-compensator W_2 was set to identity, and W_1 once again was designed such that G_s would have higher gain and low frequency. However in order to have robust stability, the bandwidth of S and T must be a little bit higher than in the additive and multiplicative cases. This was also the case

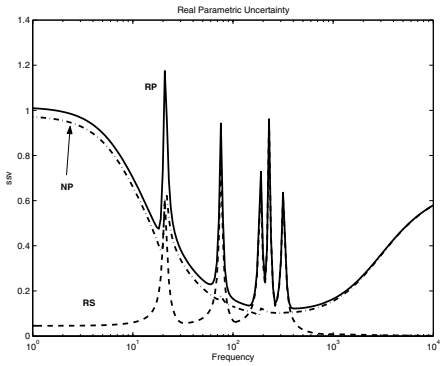

Fig. 5. SSV plots (H_∞ 2DOF design Parametric Uncertainty in ω_n)

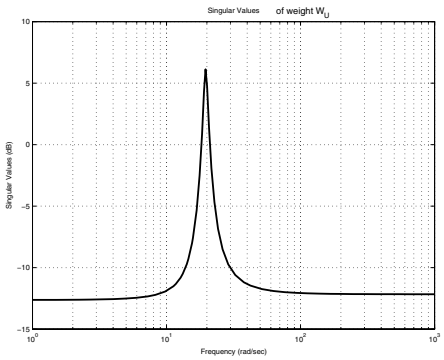

Fig. 6. Singular values of weight W_U (Multiplicative Uncertainty)

in LQG, and mixed sensitivity H_∞ designs. The diagonal pre-compensator that accomplishes this is:

$$W_1 = diag(\frac{0.065s + 1625}{s + 250})_{15\times 15} \tag{18}$$

The specified model matching parameter was $\rho = 3.6$. Solution for the two degree of freedom H_∞ controller was accomplished by gamma iteration with the final $\gamma = 4.98$. Since the pre-compensator is the same order as the additive and multiplicative designs, the resulting controller again has 44 states. This controller is then reduced to 29 states with negligible difference from the full order controller. The singular value plots of S, T, and K again satisfed the imposed constraints and were ommited to save space. The reference step response, z displacement, and control signal verses time are given in the following figures. Again are satisfactory and similar to the previous plot and thus are omitted. The structured singular value plots were constructed for 210% and 2% uncertainty in ζ_n and ω_n respectivly. These plots show that this system has nominal performance and robust stability for these uncertainty levels. When considering a combination of uncertainties in both ζ_n and ω_n these tolarable percentages would be lowered with ω_n being the most important parameter. If a robustly performing control design is required the uncertainty levels may not exceed 155% and 1.7% uncertainty in ζ_n and ω_n respectivly. The SSV plot for uncertainty in ω_n is shown in Fig. 5.

B. H_∞ Control Design

A standard mixed sensitivity H_∞ framework described in section (III-A) in was also undertaken. The advantage of this approach is the ease with which frequency domain constraints may be specified on the closed loop transfer functions. However in MIMO systems like this one the weight formulation is quite complicated. The weights used here are all diagonal which may not be the best choice. However in the literature one rarely encounters MIMO designs that use anything different, and it is often considered foolish to attempt anything more complex. The following section present the H_∞ design process and simulation results.

H_∞ Design for Input Multiplicative Uncertainty: The key part of a mixed sensitivity H_∞ design is the proper selection of weights W_p, W_U, and W_T. W_p is a bound on the closed loop sensitivity function S that determines the ability of the system to reject noise, it also and indirectly determines sets a lower bound on the tracking bandwidth of the system. Therefore the weight between each of the reference input channels to the corresponding lift and roll moment output channels was selected to be a first order transfer function with a bandwidth of 150 Hz, roll off of 20 dB per decade, a DC gain of 40 dB and a high freq gain of about -3.5 dB. Equation (19) gives the weight W_p.

$$W_p(s) = diag\{\tfrac{0.6667s+942.5}{s+9.425}, \tfrac{0.6667s+942.5}{s+9.425}, \tfrac{1000s}{s^2+3770s+3.5e6}, \cdots\} \tag{19}$$

Similarly the weight on the complementary sensitivity is chosen to place an upper bandwidth on the tracking ability of the closed loop system so as to facilitate noise rejection. This value was set at 500 Hz. This was applied to all channels for lack of a better weight for the other 15 input channels. Equation (20) gives this weight.

$$[W_T(s)]_{17\times 17} = \frac{s + 2513}{0.01s + 3142}\,[I_{17\times 17}] \tag{20}$$

Designing the weight KS is slightly more difficult. Looking at the plot of N_{ydwd} it is clear that there is a spike at approximately 20 Hz and everywhere else robust stability is satisfied. Therefore by creating a notch in KS at 20 Hz it was possible to ensure robust stability to input multiplicative uncertainty. The weight that achieves this is given in equation (21) and is shown in figure (6).

$$W_U(s) = \frac{0.2464s^2 + 3.165s + 89.61}{s^2 + 1.566s + 383.7}\,[I_{15\times 15}] \tag{21}$$

The resulting controller had a $\gamma = 1.1459$, and was 94 order. The reduced order controller had 29 states and was again nearly the same as the full controller in the important frequency range. The step response, z-displacement, and control signals were desirable values. N_{ydwd} is less than one for 25% uncertainty in the input signal. In addition the mu plots in figure (7) indicate both robust stability and nominal performance are satisfied. If robust performance is desired the controller can only tolerated 10% uncertainty in the input.

H_∞ Design for Parametric Uncertainty: The design for robust stability under parametric uncertainty was more difficult because unlike additive, and multiplicative uncertainty there was no direct way to impart frequency domain

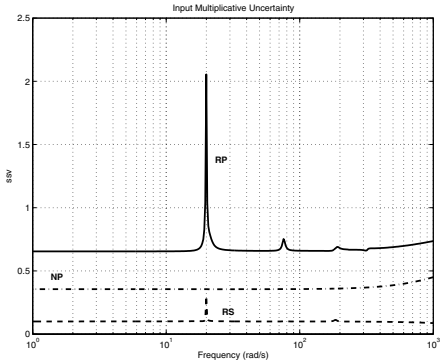

Fig. 7. SSV plots (H_∞ Multiplicative Uncertainty)

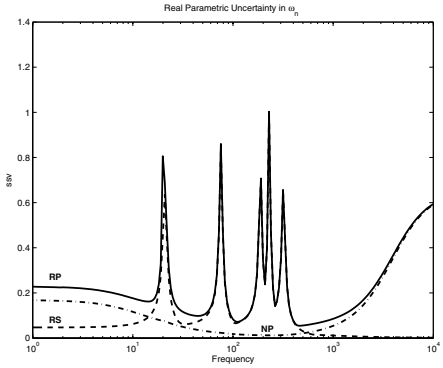

Fig. 8. SSV plots (H_∞ Parametric Uncertainty in ω_n)

constraints in the S/KS/T mixed sensitivity design. Therefore the procedure was more ad hoc‘. The complementary sensitivity weight that was most successful was a 4th order weight. The weight on KS is again a constant 15×15 weight of 1/15. Also modified from last design is the weight W_P. It is still a diagonally repeated first order weight with low frequency gain of around -40dB, a high frequency gain of 1.25, and a break frequency of around 700 Hz. The resulting controller had a $\gamma = 0.54417$, and was 80th order. After reduction to 29 states it was still indisguishable from the full order controller.

The μ-analysis for real parametric uncertainty in the plant again shows that it is difficult to satisfy robust stability and nominal performance. For the best H_∞ design the maximum amount of uncertainty in $zeta_n$ that was tolerated for robust stability was 215%. The maximum amount of uncertainty in ω_n that was tolerated for robust stability was only 2.2%. Again when considering uncertainty in both parameters simultaneously, the maximum amount uncertainty tolerated for robustness in each parameter is less than these values. If robust performance is desired the controller can only tolerate 200% uncertainty in ζ_n and 2% uncertainty in ω_n. The SSV plot for uncertainty in ω_n is shown in Fig. 8

V. CONCLUSIONS AND FUTURE WORK

The key points of comparison for these designs are the ability to provide: nominal performance, robust stability, a low order controller, and robust performance. In addition the ease and intuition with which each was designed was also considered. Under input multiplicative uncertainty, the 2 DOF H_∞ design was able to satisfy RS, NP, and RP for 25% input multiplicative uncertainty, while the other designs could only satisfy all three for lesser percentages of uncertainty. For parametric uncertainty. The mixed sensitivity H_∞ design was able to satisfy RS, NP, and RP for 2% uncertainty in ω_n or 215% in ζ_n. This was the best control design in terms of robustness, but for this particular formulation there was no direct way to design the H_∞ controller for robustness to parametric uncertainty. The 2 DOF H_∞ design was perhaps the easiest to design when compared to the others (especially the mixed sensitivity H_∞ controller). This could be that parametric uncertainty translates very well to coprime uncertainty as shown in [4]. The 2 DOF H_∞, and mixed sensitivity H_∞ were both able to achieve good robustness properties. 2%-3% uncertainty in ω_n is generally considered the maximum amount of uncertainty that controllers for structural system will typically tolerate [4]. Furthermore if uncertainty in only one or two of the natural frequencies and damping ratios is considered this tolerable percentage will likely increase.

During the course of this work a need for greater accuracy in the description of the sensors and actuators was identified. Similarly, a dynamic aeroelastic characterization with lag states would add greater realism to the model. Future avenues of work include modifications to structural model, the aerodynamic model, the control design, and the simulation. A detailed parametric investigation of more suitable and available materials for the structure needs to be undertaken. The efforts described in this paper will serve as a spring board for incorporating controller robustness analysis and synthesis for these future aeroelastic models. This ultimately will give a very good indication if this proposed morphing concept has merit for further experimental studies and possible applications.

REFERENCES

[1] Whitmer, Christopher E., et al., “Modeling and control of a morphing airfoil American Society of Mechanical Engineers, Dynamic Systems and Control Division DSC, v 72, n 2, 2003, p 829-836

[2] Kudva, et al., “The DARPA/AFRL/NASA Smart wing program - Final overview” SPIE Conference on Smart Structures and Materials, Industrial and Commercial Applications of Smart Structures Technologies, Vol. 4698, pp 37-43, 2002.

[3] Raney, David L., et al. “Flight Control Using Distributed Shape-Effector Arrays”, *AIAA Paper 2000-1560*, April 2000

[4] Aouf, Nabil, B. Boulet. “Uncertainty Models and Robust Complex-Rational Controller Design for Flexible Structures”, *Journal of Guidance, Control, and Dynamics*, Vol.26, No.4 July-August 2003

[5] Inman, D. J., et al., Aeroelastic Optimization of Adaptive Bumps for Yaw Control, Journal of Aircraft Vol. 41, No. 1, Jan-Feb 2004.

[6] Skogestad, S.; I. Postlethwaite, *Multivariable Feedback Control Analysis and Design*, John Wiley and Sons 1996.

[7] Glover, K., and D. McFarlane, *Robust Stabilization of Normalized Coprime Factor Plant Descriptions with H_∞ bounded uncertainty*, *IEEE Transactions on Automatic Control.* Vol. 34(8), pp 821-30, 1989.